

ER-localized auxin transporter PIN8 regulates auxin homeostasis and male gametophyte development in *Arabidopsis*

Zhaojun Ding^{1,2}, Bangjun Wang³, Ignacio Moreno⁴, Nikoleta Dupláková⁵, Sibin Simon¹, Nicola Carraro⁶, Jesica Reemmer⁶, Aleš Pěňčík⁷, Xu Chen¹, Ricardo Tejos¹, Petr Skůpa⁵, Stephan Pollmann⁸, Jozef Mravec¹, Jan Petrášek⁵, Eva Zažímalová⁵, David Honys⁵, Jakub Rolčík⁷, Angus Murphy⁶, Ariel Orellana⁴, Markus Geisler³ & Jiří Friml^{1,9}

Auxin is a key coordinative signal required for many aspects of plant development and its levels are controlled by auxin metabolism and intercellular auxin transport. Here we find that a member of PIN auxin transporter family, PIN8 is expressed in male gametophyte of *Arabidopsis thaliana* and has a crucial role in pollen development and functionality. Ectopic expression in sporophytic tissues establishes a role of PIN8 in regulating auxin homeostasis and metabolism. PIN8 co-localizes with PIN5 to the endoplasmic reticulum (ER) where it acts as an auxin transporter. Genetic analyses reveal an antagonistic action of PIN5 and PIN8 in the regulation of intracellular auxin homeostasis and gametophyte as well as sporophyte development. Our results reveal a role of the auxin transport in male gametophyte development in which the distinct actions of ER-localized PIN transporters regulate cellular auxin homeostasis and maintain the auxin levels optimal for pollen development and pollen tube growth.

¹ Department of Plant Systems Biology, VIB and Department of Plant Biotechnology and Genetics, Ghent University, B-9052 Gent, Belgium. ² The Key Laboratory of Plant Cell Engineering and Germplasm Innovation, Ministry of Education, School of Life Sciences, Shandong University, Shanda Nanlu 27, Jinan 250100, China. ³ Department of Biology, Plant Biology, University of Fribourg, 1700 Fribourg, Switzerland. ⁴ Center for Genome Regulation, Center of Plant Biotechnology, Facultad de Ciencias Biológicas, Universidad Andres Bello, Santiago, Chile. ⁵ Institute of Experimental Botany ASCR, 16500, Praha 6, Czech Republic. ⁶ Department of Horticulture, Purdue University, West Lafayette, Indiana, USA. ⁷ Laboratory of Growth Regulators, Centre of the Region Haná for Biotechnological and Agricultural Research, Faculty of Science, Palacký University, 78371 Olomouc, Czech Republic. ⁸ Ruhr-Universität Bochum, Lehrstuhl für Pflanzenphysiologie, 44801 Bochum, Germany. ⁹ Department of Functional Genomics and Proteomics, Faculty of Science, and CEITEC, Masaryk University, Kamenice 5, CZ-62500 Brno, Czech Republic. Correspondence and request for materials should be addressed to J.F. (e-mail: jiri.friml@psb.vib-ugent.be).

The plant hormone auxin has a crucial role in plant development¹⁻⁶. On account of its differential distribution within plant tissues, it acts as a versatile coordinative signal mediating a multitude of processes, including female gametophyte patterning, embryogenesis, organogenesis, meristem activity, growth responses to environmental stimuli and others⁷⁻¹⁰. High auxin concentration in germinating pollen and active auxin responses in developing pollen¹¹⁻¹³ implicated auxin also in male gametophyte development and function, but its role there remained elusive.

A crucial aspect of auxin action is its graded distribution (auxin gradients) that depends on local auxin biosynthesis¹⁴⁻¹⁶ and directional, intercellular auxin transport^{7,17,18}. The polar auxin transport has an essential role in most auxin-regulated processes and is mediated by auxin influx proteins from the AUX1/LAX family¹⁹, by PIN auxin efflux proteins²⁰ and by homologues of the ABCB multiple drug resistance transporters^{21,22}. These auxin transporters typically localize to the plasma membrane (PM) and facilitate auxin flow across the membrane in and out of the cell²³. Recently, the *Arabidopsis thaliana* PIN5 auxin transporter has been shown to localize to the endoplasmic reticulum (ER) and its activity is important for the regulation of auxin metabolism²⁴. These findings suggest the existence of auxin transport across the ER membrane, although a demonstration of such transport has not been provided yet and its role in auxin biology and plant development is still largely unclear.

Here we identify and functionally characterize PIN8, an auxin transporter preferentially expressed in male gametophyte. PIN8 transports auxin across the ER membrane and antagonistically to PIN5 regulates intracellular auxin homeostasis and metabolism for male gametophyte function.

Results

PIN8 is expressed and functions in the male gametophyte.

To assess a potential role for the auxin transport in male gametophyte development, we examined the expression patterns of PIN auxin transporters by using available transcriptome data²⁵. Among the eight members of the PIN protein family in the *Arabidopsis* genome, a so-far uncharacterized member PIN8 was the only one predominantly expressed in pollen (Supplementary Fig. S1a). Reverse transcription PCR confirmed the highly enriched expression of PIN8 in reproductive tissues (Supplementary Fig. S1b) and lines comprising the *PIN8* coding region fused with green fluorescent protein (GFP) under the control of its native promoter (*PIN8::PIN8-GFP*) showed strong signal in developing and germinating pollen (Supplementary Fig. S1a).

To analyse the potential role of PIN8 in pollen development, we isolated two insertion mutant alleles, *pin8-1* and *pin8-2*, disrupting the first and fifth exon of the *PIN8* gene, respectively (Supplementary Fig. S1c,d). No obvious phenotypic defects were observed in seedlings and adult plants in both alleles (data not shown), which was consistent with very low *PIN8* expression in most sporophytic tissues. However, *pin8* mutants showed a decreased transmission ability through male gametophyte (38%) for *pin8-1* versus the expected 50% for the wild-type (Col-0) pollen (Fig. 1a). The complementation of this phenotype confirmed that the described pollen transmission defects are due to the loss of PIN8 function (Supplementary Fig. S2). 4',6-Diamidino-2-phenylindole (DAPI) staining analysis revealed a high frequency of aborted and misshaped pollen grains in *pin8* (Fig. 1b,c, Supplementary Table S1) and transmission electron microscopy analyses showed that *pin8* mutant pollen has a reduced density of rough ER (10–15%, $n > 150$ pollen grains) in comparison to the wild-type pollen (Fig. 1d,e). Next, we examined transgenic lines overexpressing *PIN8* under strong pollen-specific promoter *LAT52* (ref. 24). *LAT52::PIN8* also showed strongly reduced transmission through the male gametophyte (below 10% for *LAT52::PIN8* versus expected 50% for the wild-type control; Fig. 1a and Supplementary Fig. S1e). In addition, *in vitro*

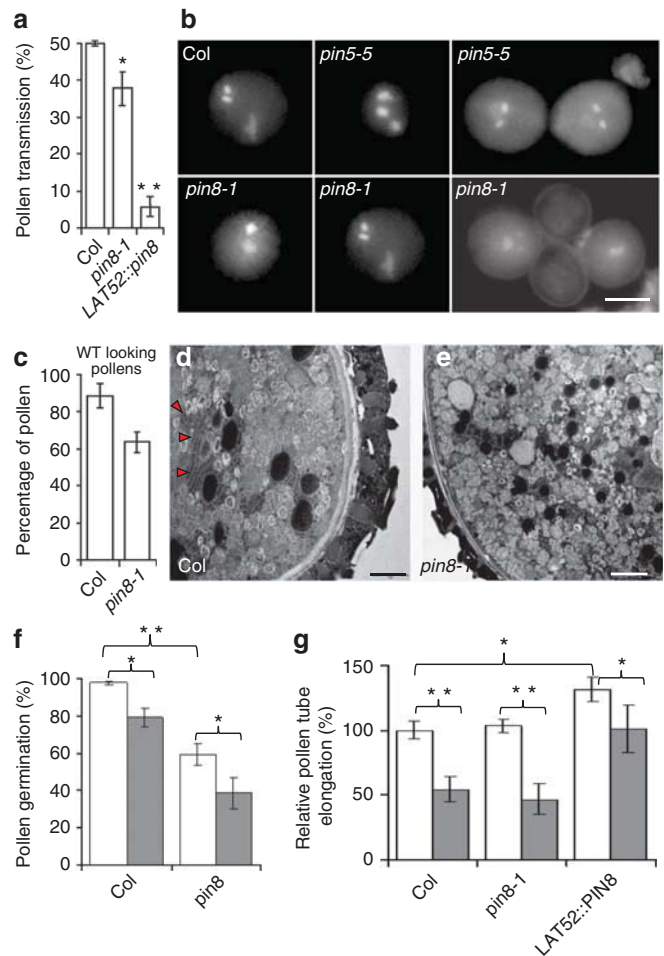


Figure 1 | PIN8 is involved predominantly in the male gametophyte development.

(a) The *pin8* mutant and the *LAT52::PIN8* line showed reduced pollen transmission ability. Error bars represent the standard error of more than ten independent crosses (Student's *t*-test, * $P < 0.05$). (b,c) DAPI staining analysis showing defects in the morphology of *pin8* and *pin5* mutant pollen. Both mutants showed distorted and/or misplaced male germ unit and less frequently also exhibit pollen mitosis defects. Sometimes, collapsed pollen grains were observed. Scale bar, 10 μ m. Error bars represent the standard error of more than 23 independent plants (Student's *t*-test, ** $P < 0.01$). (d,e) Typical ER clusters in wild-type (WT) pollen (d) were not observed in 10–15% *pin8* pollen (observed 150 pollen grains) (e) by transmission electron microscope analysis. Scale bar, 10 μ m. Red arrows mark ER clusters. (f) *pin8* (2256 pollen were analysed) shows reduced *in vitro* pollen germination abilities (2,814 Col pollens were analysed as the control) and increased sensitivity to auxin treatment (100 nM NAA) with a 35% reduction of pollen germination in *pin8* (5,017 pollens were analysed) compared with the 19% reduction in Col (1,131 pollens were analysed). Error bars represent the standard error of more than ten independent plants (Student's *t*-test, * $P < 0.05$; ** $P < 0.01$). White and grey columns represent without and with NAA treatment, respectively. (g) Overexpression of *PIN8* in pollen in the *LAT52::PIN8* line strongly increased the resistance (with a 24% inhibition of pollen tube length compared with the 46% inhibition in Col) of *in vitro* pollen germination to NPA (100 μ M NPA) treatment. Error bars represent the standard error of more than six independent plants (Student's *t*-test, * $P < 0.05$; ** $P < 0.01$). White and grey column represent without and with NPA treatment, respectively, in Col, *pin8* or *LAT52::PIN8*.

pollen germination assays revealed a decreased pollen germination in *pin8* (40% decrease, Fig. 1f) and increased pollen tube elongation in *LAT52::PIN8* lines (30% increase, Fig. 1g) with a normal pollen

tube morphology (Supplementary Fig. S1f). Thus, the loss-of-function and ectopic expression analyses revealed a specific role of PIN8 in male gametophyte development and function.

As PIN8 is a member of the auxin transporter family, it is presumably involved in auxin transport. However, a role of auxin transport in male gametophyte development and function is far from being clear. To address this issue, we pharmacologically manipulated auxin levels and auxin transport during pollen germination and pollen tube growth. Auxin treatments (100 nM α -naphthaleneacetic acid (NAA)) reduced the pollen germination rate in wild type (19% reduction) and *pin8-1* pollen showed increased sensitivity to such auxin treatment (35% reduction) (Fig. 1f). Furthermore, the auxin transport inhibitor 1-*N*-naphthylphthalamic acid (NPA) strongly inhibited pollen tube growth and, notably, *LAT52::PIN8* pollen showed increased resistance to this NPA effect (Fig. 1g). The inhibition of the *in vitro* pollen tube growth by NPA was apparent only at high concentrations (100 μ M) indicating that it might occur through APM1-regulated functions of PIN and ABCB auxin transport proteins, as APM1 is the target at high concentrations of NPA treatment^{26,27}. The change in sensitivity in pollen tubes overexpressing auxin transport-related protein PIN8 suggests that it is auxin transport-related effect of NPA that affects pollen tube growth. Collectively, these findings hint at an important role of auxin and auxin transport for male gametophyte function and identified the pollen-specific putative auxin transporter PIN8 as an important factor regulating these processes.

PIN8 overexpression affects many aspects of plant growth and development. To further characterize the function of PIN8, we generated lines overexpressing PIN8 in sporophytic tissues under the control of the strong cauliflower mosaic virus 35S promoter (*PIN8OX*). *PIN8OX* lines flowered much earlier than wild-type plants (Fig. 2a,b), showed enhanced leaf margin serration, especially under short-day growth conditions (Fig. 2c) and had much longer hypocotyls than the control (Fig. 2d,e), which can be attributed to the increased cell elongation (Fig. 2f and Supplementary Table S2). All these plant growth and development phenotypes in *PIN8OX* suggest a capacity of PIN8 to influence different aspects of plant development, preferentially those where auxin is involved.

PIN8 and PIN5 localize to the ER. In *Arabidopsis*, the PIN auxin transporter family can be divided in two subclades: one represented by PIN1, PIN2, PIN3, PIN4 and PIN7, which all localize to the PM²³, and the other subclade represented by PIN5, PIN8 and possibly PIN6, which are characterized by a reduced middle hydrophilic loop²³ and for which PIN5 has been shown to localize to the ER in *Arabidopsis*²⁴. To investigate the subcellular localization of PIN8, we examined *Arabidopsis* transgenic lines expressing a functional *PIN8::PIN8-GFP* construct. In *PIN8::PIN8-GFP* (Supplementary Fig. S2), a specific intracellular signal was observed only in pollen and growing pollen tubes (Fig. 3a–c and Supplementary Fig. S1a) consistent with the PIN8 expression data (Supplementary Fig. S1a). The *PIN8-GFP*-expressing cells showed intracellular signals, but no localization to the PM (Fig. 3a–c). A pronounced co-localization with the ER-tracer dye²⁴ suggested the association of PIN8-GFP with the ER (Fig. 3a–c).

To examine the PIN8 localization in more detail and in different sporophytic cell types, we ectopically expressed *PIN8* fused with GFP under the control of 35S promoter. Similar to what was observed in pollen, we detected a consistent, intracellular PIN8-GFP signal co-localized with ER markers, such as BIP2 (ref. 28) in root cells (Fig. 3d–f, p). On the other hand, we did not observe any co-localization of PIN8 with endosomes or Golgi apparatus (Fig. 3g–i, p and Supplementary Fig. S3) and also we did not observe any co-localization with labelled PM (Fig. 3j–l, p). Furthermore, PIN8 co-localized with PIN5 at the ER (Fig. 3m–p) and this

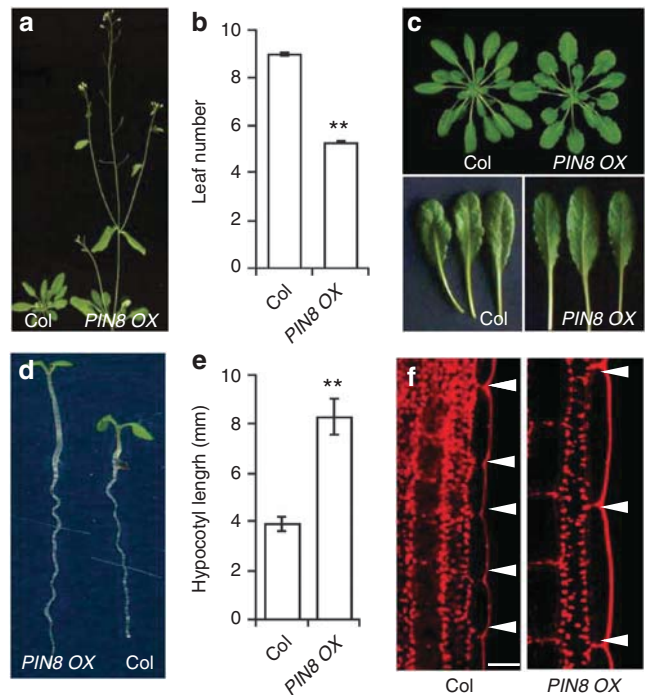


Figure 2 | *PIN8OX* lines showed defects in many aspects of plant growth and development. (a,b) *PIN8OX* lines flower earlier than the wild-type controls measured under long-day growth conditions. Error bars represent the standard error of the mean from three independent experiments ($n = 48$, Student's *t*-test, ** $P < 0.01$). (c) *PIN8OX* lines showed strongly enhanced leaf margin serration under short-day growth conditions. (d,e) *PIN8OX* lines showed long hypocotyls compared with the control. Hypocotyl length was measured with 5-day-old seedlings grown under short days. Error bars represent the standard error of the mean from three independent experiments ($n = 30$, Student's *t*-test, ** $P < 0.01$). (f) The cell length in *PIN8OX* lines is more than two times longer than that in the control (see the quantification data in Supplementary Table S2). The arrows indicate the intercellular space. Scale bar, 10 μ m.

localization was, similar to that of PIN5 (ref. 24), insensitive to the treatment with the vesicle trafficking inhibitor brefeldin A (Supplementary Fig. S4). These results strongly suggest that PIN8, similar to PIN5, localizes to the ER and that these proteins might have related functions.

PIN8 transports auxin and regulates cellular auxin homeostasis. The ER-localized PIN5 was found, in contrast to PM-localized PIN proteins, not to act in intercellular auxin transport, but to be involved in regulating cellular auxin homeostasis, presumably by compartmentalizing auxin between the ER and the cytosol²⁴. Therefore, we tested the role of PIN8 in regulating auxin homeostasis. The visualization of auxin responses with the auxin-responsive reporter *DR5::GUS*²⁹ revealed no changes in *pin8* mutants (data not shown), consistent with a very low expression of *PIN8* in sporophytic tissues. In contrast, *PIN8OX* lines showed a markedly increased *DR5* activity, both in the root and in the aerial parts of the seedling (Fig. 4a) suggesting elevated auxin levels.

To directly test the role of PIN8 in regulating auxin levels, we measured free auxin (indole-3-acetic acid (IAA)) levels in the *pin8* mutant and *PIN8OX* lines. Unfortunately, free IAA measurements directly in pollen were technically impossible, therefore, we used extraction and gas chromatography/mass spectroscopy detection of IAA in root tips, hypocotyls and rosette leaves. These measurements revealed that loss-of-function *pin8* mutants had similar levels

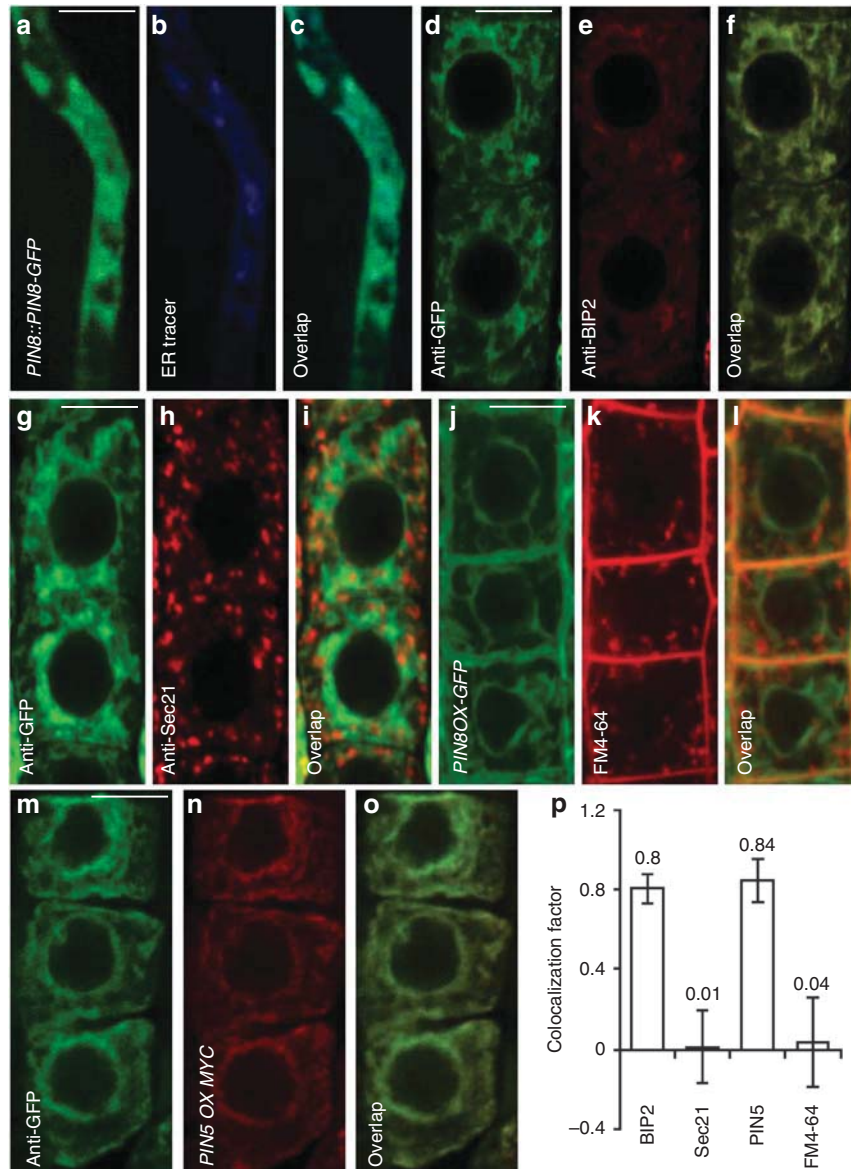


Figure 3 | PIN8 localizes to the ER. (a-c) PIN8 localization in the pollen tube of *PIN8::PIN8-GFP* line and co-localization of PIN8-GFP (green) with the ER-tracker dye (blue). (d-f) PIN8 localization in the root of *35S::PIN8-GFP* line and co-localization of PIN8-GFP (green) with ER marker BIP2 staining (red). (g-i) PIN8-GFP (green) does not co-localize with Golgi apparatus (GA) marker Sec21 (red). (j-l) PIN8-GFP (green) does not co-localize with endosomes stained with FM4-64 traced (red). (m-o) PIN8-GFP (green) and PIN5-myc (red) co-localize at the ER. (p) The quantification of PIN8 co-localization with ER (anti-BIP2), GA (anti-Sec21), PIN5 (anti-myc) and endosome (FM4-64 staining) markers confirms localization of PIN8 to the ER but not to the GA, endosomes or plasma membrane. The co-localization factor (the highest is 1.0) was calculated by Zeiss software. For microscope observation, 3-day-old seedlings ($n = 6$) and at least five areas were analysed for each seedling. Scale bar, 5 μm . Error bars represent the standard error. Live cell imaging (a-c, j-l) and immunostainings (d-f, g-i, m-o).

of free auxin as the control (Fig. 4b), whereas *PIN8OX* lines showed strongly increased free IAA levels in root tips, hypocotyls and rosette leaves (Fig. 4b). Thus, both DR5-monitored auxin response and direct auxin measurements revealed overall elevated auxin levels in plants overexpressing *PIN8*.

Next, we quantified the auxin efflux from mesophyll protoplasts isolated from rosette leaves of *PIN8* loss-of-function and overexpression lines. Consistent with the changes in auxin levels and *PIN8* expression data, protoplasts prepared from *pin8* mutants exhibited a comparable IAA and NAA efflux as wild-type controls, whereas in protoplasts isolated from *PIN8OX*, the efflux of IAA and NAA was increased (Fig. 4c and Supplementary Fig. S5), suggesting the

auxin transport competence of PIN8. The ER localization of PIN8 in protoplasts (Supplementary Fig. S6) is also consistent with a notion that PIN8 increases efflux of auxin from the ER into the cytoplasm and then presumably out of the protoplast.

To directly assess the ability of PIN8 at the ER membranes, we grew *PIN8OX*-etiolated plants in liquid culture and ER-enriched membrane fractions were prepared using sucrose gradient centrifugation as described³⁰. This fraction was well separated from non-ER fractions including Golgi membranes and other organelles. PIN8-GFP was detected in the ER-enriched fraction with an anti-GFP antibody, but no PIN1 was detected with anti-PIN1 (not shown) confirming no or very low PM contamination. Transport assays with

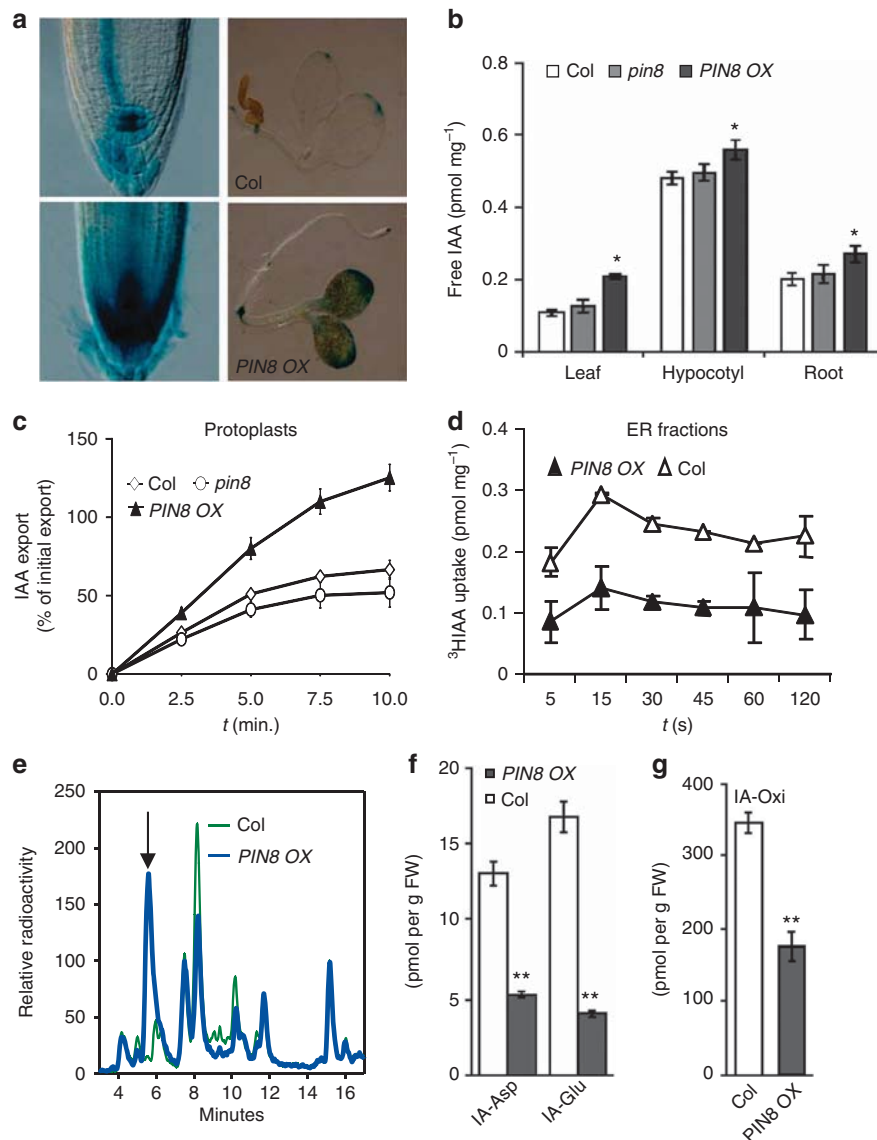


Figure 4 | PIN8 regulates cellular auxin homeostasis and auxin transport. (a) *PIN8OX* exhibits enhanced auxin response as shown by the increased *DR5::GUS* activity in the root and in the aerial parts of the seedling. (b) Changes in free IAA levels in *PIN8OX* in young leaves/cotyledons, hypocotyls and root tips. Error bars represent the standard error of the mean, $n=5$ (Student's *t*-test, * $P < 0.05$). (c) Protoplasts of *PIN8OX* showed a higher rate of IAA export. Error bars represent the standard error of the mean, $n=3$. (d) ³H-IAA uptake time course in ER-enriched membrane fractions from Col and *PIN8OX* plants. Transport assays were performed as described in Methods. ER-enriched membranes were incubated in 50 nM ³H-IAA fractions. Aliquots were taken at different times, filtered and washed. The radioactivity present in the filters was estimated by liquid scintillation counting and expressed as pmol of ³H-IAA/mg of total proteins. The experiment was performed two biological repeats, and the error bars represent the standard error of the mean. (e) The HPLC chromatogram of IAA metabolic profile changes noticeably in the *PIN8OX* line compared with the wild-type control (2.5-h incubation with ³H-IAA). (f,g) Liquid chromatography/mass spectrometry detected strongly decreased levels of IAA conjugates (indole-3-acetyl-aspartate, IA-Asp; indole-3-acetyl-glutamate, IA-Glu) (f), and oxindole-3-acetic acid (OxIAA) (g) in *PIN8OX* line. White and grey column represent Col and *PIN8OX*, respectively. Error bars represent the standard error of the mean, $n=3$ (Student's *t*-test, ** $P < 0.01$). FW, fresh weigh.

radiolabelled IAA showed increased auxin accumulation capacity of the ER fractions from the *PIN8OX* lines as compared with the control (Fig. 4d). In addition, competitive uptake assays with ER-enriched fraction from *PIN8OX* revealed that synthetic auxins NAA, 2,4-D and auxin analogue indole-3-butyric acid can compete with radiolabelled IAA uptake, whereas the biologically inactive analogue benzoic acid (1 mM) did not compete with PIN8-mediated uptake of radiolabelled IAA (Supplementary Fig. S7a). Our auxin transport assays in mesophyll protoplasts from transiently transfected *nicotiana benthamiana* also indicated that IAA, not benzoic acid, was the preferred substrate of PIN8 action (Supplementary Fig. S7b).

These results show that IAA and other biologically active auxins are preferred substrates of PIN8 action. In an independent set of experiments, lighter ER membranes from *PIN8OX* seedlings, exhibited acidification after addition of ATP and accumulation of ³H-IAA in short-term (60 s) uptake assays, whereas denser ER vesicles, tonoplast vesicles and PM vesicles did not show auxin transport activity (Supplementary Fig. S8). The overall increase in auxin responses and free auxin levels in *PIN8OX* as well as changed auxin transport capacity of *PIN8OX* protoplasts and ER-derived membranes altogether suggested that PIN8 is an ER-localized auxin transporter involving in the regulation of auxin homeostasis.

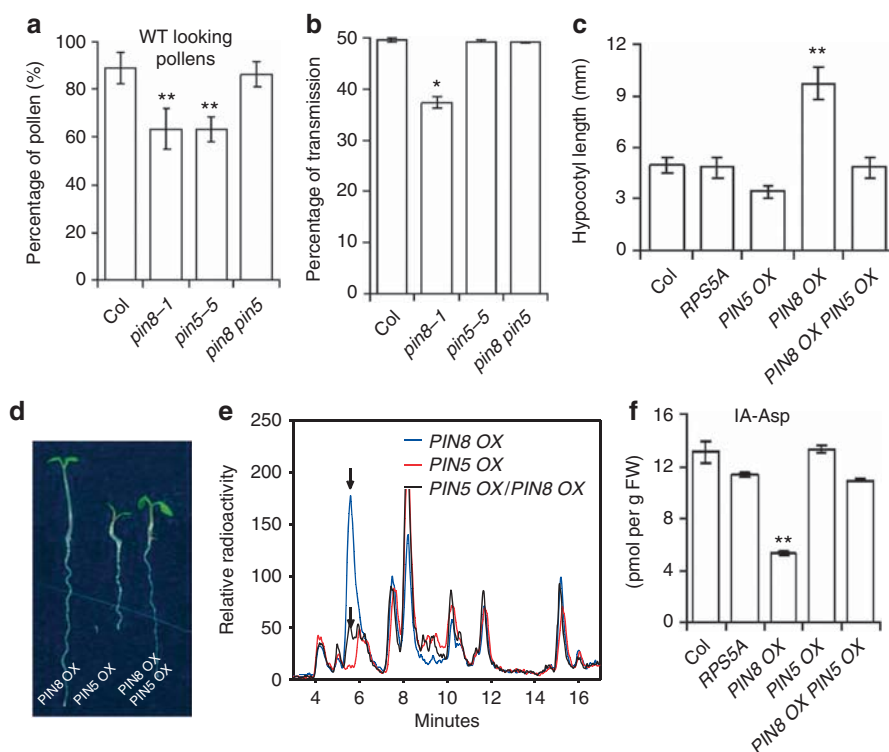


Figure 5 | PIN8 and PIN5 act antagonistically. (a) Morphological defects in pollen of *pin5* (2,400) and *pin8* (2,400) single mutants were rescued in *pin5 pin8* (3,300) double mutants as shown by DAPI staining. A total of 7,100 wild-type (WT) pollens were counted as the control. Error bars represent the standard error of more than 23 independent plants (Student's *t*-test, ***P* < 0.01). (b) The reduced pollen transmission ability in the *pin8* mutant was rescued in the *pin5 pin8* double mutant. Error bars represent the standard error of more than ten independent crosses (Student's *t*-test, **P* < 0.5). (c,d) The long hypocotyl phenotype of the *PIN8OX* line was rescued in the *PIN8OX PIN5OX* line. Error bars represent the standard error of three independent experiments (*n* = 60, Student's *t*-test, ***P* < 0.01). (e) Specific HPLC chromatogram of IAA metabolic profile of *PIN8OX* was largely rescued in the *PIN8OX PIN5OX* line (2.5-h incubation with ³H-IAA). Arrows indicate the notable changes in the IAA metabolic profile. (f) The decreased IA-Asp of the *PIN8OX* line was rescued in the *PIN8OX PIN5OX* line. Error bars represent the standard error of the mean, *n* = 3 (Student's *t*-test, **P* < 0.05).

To assess the role of PIN8 in IAA metabolism, we analysed the IAA metabolic profile of *PIN8OX* transgenic seedlings through high-performance liquid chromatography (HPLC). *PIN8* overexpression remodelled the IAA metabolism as demonstrated by the pronounced changes in the HPLC profile (Fig. 4e). Direct analysis by ultra-high-performance liquid chromatography coupled to tandem mass detection of the selected IAA conjugates confirmed the changes in the IAA metabolic profile and showed that the *PIN8OX* line had a decreased capacity to produce amino-acid conjugates, such as IA-Asp (indole-3-acetyl-aspartate), IA-Glu (indole-3-acetyl-glutamate) or OxIAA (oxindole-3-acetic acid; Fig. 4f,g). These results demonstrated that the ER-localized PIN8 auxin transporter, similar to PIN5, is also involved in the regulation of auxin homeostasis.

PIN8 and PIN5 act antagonistically. To gain additional insights into the roles of PIN5 and PIN8, we systematically compared the loss-of-function and overexpression lines and also generated the *pin5 pin8* double mutants and the *PIN8OX PIN5OX* double transgenic plants. Similar to *pin8*, *pin5* was also defective in pollen morphology (Figs 1b, 5a), but, in contrast to the single *pin5* mutant, the *pin5 pin8* double mutant largely rescued the pollen morphology defects and the *pin8* defect in transmission through the male gametophyte (Fig. 5a,b). Thus, the *pin5* and *pin8* loss-of-function mutants compensated to a large extent each other in male gametophyte development and function.

Regarding the overexpression lines, *PIN5OX* seedlings had shorter hypocotyls²⁴, whereas *PIN8OX* seedlings had strikingly

longer hypocotyls than the wild-type control (Fig. 5c,d). These overexpression effects were also rescued in the *PIN8OX PIN5OX* double overexpressing line (Fig. 5c,d). In addition, we also observed that *pin5* significantly enhanced the long hypocotyl phenotype of *PIN8OX* further supporting the antagonistic roles of PIN5 and PIN8 (Supplementary Fig. S9a). The same could be observed for the flowering time. Under long-day conditions, *PIN8OX* plants flowered earlier than the control, whereas *PIN5OX* plants flowered significantly later (Supplementary Fig. S9b,c) and the *PIN8OX PIN5OX* plants flowered at a time that was comparable to the control plants (Supplementary Fig. S9b,c). These different observations are also consistent with previous observations on the opposite action of PIN5 and PIN8 in root hair development³¹. Thus, both the loss-of-function mutants and overexpression lines of *PIN5* and *PIN8* can largely compensate each other in regulating different developmental processes, suggesting antagonistic roles of these two ER-localized PIN proteins.

Next, we tested genetic interaction between PIN5 and PIN8 in regulating auxin homeostasis. In the *PIN8OX* line, both free IAA measurements and enhanced *DR5::GUS* activity consistently suggested increased free IAA levels (Fig. 4), whereas *PIN5OX* had been shown to have decreased auxin levels²⁴. To test the possible antagonistic roles of PIN5 and PIN8 in the regulation of auxin metabolism, we measured free IAA levels in *PIN8OX PIN5OX* double transformants. This analysis revealed that, similar to morphological phenotypes, the increased free IAA levels in *PIN8OX* were largely rescued in the *PIN8OX PIN5OX* line that exhibited free IAA levels

comparable to those of the control lines (Supplementary Fig. S10a). The increased IAA export in protoplasts prepared from *PIN8 OX* also phenocopies *pin5* mutant (Supplementary Fig. S10b). Moreover, notable changes in the IAA metabolic profile of *PIN8OX* seedlings as demonstrated by the HPLC spectrum were also largely rescued in *PIN8OX PIN5OX* lines (Fig. 5e). Accordingly, liquid chromatography–tandem mass spectrometry analysis confirmed that the decreased capacity of *PIN8OX* seedlings to conjugate IAA to amino acids was rescued in the *PIN8OX PIN5OX* lines (Fig. 5f).

Overall, the opposite and mutual compensatory effects of *pin5* and *pin8* loss-of-function and overexpression alleles on male gametophyte and sporophyte phenotypes as well as on auxin homeostasis and metabolism revealed that PIN5 and PIN8 act antagonistically. This strongly suggests that PIN5 and PIN8 localized both at the same subcellular compartment (ER) can have distinct roles.

Discussion

In conclusion, this study identified auxin transporter PIN8 with a strong expression in a male gametophyte and revealed a role for auxin transport in regulating pollen development and function. Our results, including localization, auxin transport as well as genetic and physiological analyses, showed that, although both PIN8 and PIN5 auxin transporters are localized at the ER, they can have antagonistic roles in regulating gametophyte and sporophyte development, cellular auxin homeostasis and metabolism. PIN5 has been proposed to transport auxin intracellularly from the cytoplasm into the ER, where enzymes involved in IAA metabolism are compartmentalized⁶, thus reducing the auxin availability for the PM-based auxin efflux²⁴. It is unclear how PIN8 localized to the same intracellular compartment, namely ER, can act antagonistically but it suggests more complex functional interaction between PIN proteins than anticipated so far. A possible scenario would envision transient or more stable interaction of PIN5 and PIN8 negatively regulating each other transport capabilities. Notably, PIN8 activity in *Arabidopsis* is required only in male gametophyte. It is known that developing and germinating pollen has high levels of auxin³², but the auxin role there is unclear. Thus, it is possible that specifically during pollen development, the ER-localized PIN transporters regulate the release of auxin from the internal stores in the ER to drive auxin-mediated pollen tube elongation.

The finding that some PIN proteins localize to the ER and other to the PM brings about an interesting question, namely, which of these functions and cellular localizations is ancestral and which physiological and developmental role did this ancestral PIN protein play. In the moss *Physcomitrella*, the most typical member of PIN clade localizes to ER, when expressed in BY-2 tobacco cells²⁴. As in most ancestral land plants, the gametophyte generation is predominant, the male gametophytic PIN8 might represent a more ancestral form of auxin transporters that were at the ER involved in regulating subcellular auxin homeostasis, before they acquired PM localization and new function in mediating auxin transport between cells for mediating development of higher plants. Nonetheless, also in higher plants, different ER-localized PIN proteins, including *Arabidopsis* PIN5, PIN8 and possibly also PIN6, have spatially and/or temporally distinct expression patterns²⁴ that can fine-tune the cellular free IAA levels optimal for plant growth and reproduction.

Methods

Plant material and DNA constructs. For all experiments, we used *Arabidopsis thaliana* ecotype Columbia (Col). Insertion mutant lines were *pin5-5* (ref. 24), *pin8-1* (Salk_107965) and *pin8-2* (Salk_044651). Transgenic lines were *DR5::GUS²⁹*, *DR5rev::GFP³³*, *RPS5A::GALA* (ref. 34) and *RPS5A >> PIN5-myc (PIN5 OX)*²⁴. *pin5 pin8* double mutants and the *PIN8OX PIN5OX* double transgenic plants were generated through crossing *pin5-5* with *pin8-1* or crossing *PIN8OX* with *PIN5OX*. All SALK lines were obtained from the Nottingham Arabidopsis Stock Center. The *35S::PIN8-GFP (PIN8 OX)* line was generated by

transformation of the ecotype Columbia (Col) with the *35S::PIN8-GFP (PIN8OX)* construct²⁴. The *LAT52ΔPIN8* line was generated via replacing the *35S* promoter with the *LAT52* promoter and transformed to the *Colecotypte*. The primers used for cloning the *LAT52* promoter are described in Supplementary Table S3.

Growth conditions. Seeds were sterilized with chlorine gas and stratified at 4°C for 3 days in the dark. Seedlings were grown vertically on half Murashige and Skoog (MS) medium supplemented with 1% sucrose and respective drugs. Drugs were purchased from Sigma-Aldrich. Plants were grown under the stable long-day (16h light/8h dark) or short-day (8h light/16h dark) conditions at 19°C in growth chambers.

Phenotype analyses and GUS (β-glucuronidase) staining. Plates were scanned on a flat-bed scanner and hypocotyl lengths were measured with the ImageJ (<http://rsb.info.nih.gov/ij/>) software. GUS staining was done as described³⁵.

Microscopy analysis. The immunological analyses were done as previously described³⁶. Details on antibodies and dilutions can be found in the later section. GFP samples were scanned without fixation. For confocal microscopy images, Zeiss LSM 510 or Olympus FV10 ASW confocal scanning microscopes were used.

Pollen transmission assays. We used the *PIN3::PIN3-GFP* line for the transmission wild-type controls. Pollen from the hetero *PIN3::PIN3-GFP*, hetero *pin8-1* or hetero *LAT52::PIN8* was used as a pollen donor, and crossed with Col female. Wild-type control—here is the hetero *PIN3::PIN3-GFP* line—showing around 50% transmission that was confirmed via antibiotic selection of the resulted seedlings. *pin8-1* and *LAT52::PIN8* transmission was assessed by PCR analysis or antibiotic selection of the resulted seedlings.

Auxin measurements and transport assays. Free IAA measurements and IAA metabolic profiling were done as described²⁴. For protoplast transport assays, protoplasts prepared from loss-of-function mutant and overexpression lines were loaded under controlled conditions (loading is performed on ice in order to minimize transport processes with identical amounts of cells and radioactivity) leading to highly comparable loading of cells²². Loaded cells were then temperature shifted to 25°C enabling catalysed auxin transport (of course both over the ER and PM membrane), and after defined time-points supernatants (containing effluxed radioactivity) were separated from cells by silicon oil centrifugation and quantified. For IAA conjugate quantification, ~10 mg of plant material was taken for analysis. The samples were processed as described³⁷ and quantified by ultra-high-performance liquid chromatography coupled to tandem mass detection.

Auxin transport assays in ER-enriched microsomal fractions. *Arabidopsis* plants grown in liquid culture were homogenized using razor blade in 5 ml of 0.5 M sucrose, 0.1 M KH₂PO₄ (pH 6.65), 5 mM MgCl₂ and 1 mM dithiothreitol (freshly added). Membranes were separated following the procedure described by Muñoz *et al.*^{38,39}. Briefly, the homogenate was filtered through miracloth (Calbiochem) and centrifuged at 3,000 g for 3 min. The supernatant was then layered on 5 ml of a 1.3 M sucrose cushion and centrifuged at 108,000 g for 90 min. The upper phase was removed without disturbing the interface fraction and sucrose layers of 1.1, 0.7 and 0.25 M were overlaid on the membrane pad. The discontinuous sucrose gradient was then centrifuged at 108,000 g for 90 min. The 1.1/1.3 M interface enriched in ER membranes was collected, diluted and centrifuged separately at 108,000 g for 50 min, the pellet was resuspended in 200 μl of 0.5 M sucrose, 0.1 M KH₂PO₄ (pH 6.65) and 5 mM MgCl₂ and stored at –80°C until use.

ER-enriched membranes, obtained as described above, were used to perform [³H]-IAA uptake assays, based in a filtration method previously described³⁹. A total of 50 μg of protein from the ER-enriched membrane fraction were resuspended in a buffer containing 250 mM sucrose, 20 mM KCl, 25 mM Tris-HCl (pH 7). The reaction was initiated by adding 100 μl of 50 nM [³H]-IAA (20 nCi), to reach 1 ml, final volume. Aliquots were taken at different times and filtered through 0.45-μm cellulose-ester filters (Millipore), previously treated with 250 mM sucrose, 20 mM KCl, 25 mM Tris-HCl (pH 7) and 1 mM IAA. The reaction was stopped by filtering and immediate wash using 5 ml of ice-cold 250 mM sucrose, 20 mM KCl, 25 mM Tris-HCl (pH 7) and 1 mM IAA. The filters were air-dried and the remaining radioactivity was measured in a liquid scintillation counter. The uptake of [³H]-IAA is reported in 'nmol of [³H]-IAA/mg of protein'.

Whole-mount immunolocalization and lifetime confocal microscopy. Whole-mount immunological staining on 4-day-old seedlings was done in an Intavis robot. Antibodies were used at the following dilutions: rabbit anti-BIP2 (Hsc70), 1:200 (Stressgen Bioreagents); mouse anti-GFP, 1:600 (Roche); rabbit anti-myc, 1:600 (Sigma-Aldrich). Anti-rabbit and anti-mouse antibodies conjugated with Cy3 or fluorescein isothiocyanate (Dianova, Germany) were used at 1:600 dilutions. For ER-tracker dye labelling, *PIN8::PIN8-GFP* seedlings were mounted in water with a 1:1,000 dilution of ER-tracker dye (Invitrogen). Brefeldin A treatment for 2h was performed by incubation of 4-day-old etiolated seedlings on solid MS medium supplemented with brefeldin A (50 μM), counterstaining of cell walls was achieved by mounting seedling roots in 10 μM propidium iodide.

Quantitative PCR analysis. RNA was extracted with the Plant RNeasy kit (Qiagen). Poly(dT) complementary DNA was prepared from flower total RNA. Superscript III reverse transcription (Invitrogen) and quantification were done on a LightCycler 480 apparatus (Roche Diagnostics) with the SYBR Green I Master kit (Roche Diagnostics), according to the manufacturer's instructions. All individual reactions were done in triplicate. Data were analysed as described before⁴⁰. The primers used to quantify gene expression levels are provided in Supplementary Table S3.

Light and fluorescent microscopy. For pollen phenotype observations, flowers from *pin* or Col-0 plants were collected to GUS buffer (0.1 M phosphate buffer, pH 7.0; 10 mM EDTA, pH 8.0; 0.1% triton X-100) supplemented with 100 ng ml⁻¹ DAPI as described⁴¹. After 30-min incubation at room temperature in the dark, samples were analysed by bright-field and fluorescence microscopy with Nikon TE2000-E microscope (objective Nikon CFI Plan Fluor ELWD 10×/0.60, eyepiece Nikon CFI 10×/22, intermediate magnification ×1–×1.5; Nikon).

Pollen germination *in vitro*. Pollens were collected from flowers opened day (day 0) of Col and *pin8-1* plants. Subsequently they were germinated on a germination medium on a microscope slide according to Boavida and McCormick⁴². Pollen germination medium was always prepared fresh from 0.5 M stock solutions of the main components (5 mM KCl, 0.01% H₃BO₃, 5 mM CaCl₂, 1 mM MgSO₄) using autoclaved water. Sucrose (10%) was added and pH was adjusted to 7.5 with NaOH. Low-melting agarose (Amresco, Solon, OH) was added to final 1.5% concentration and melted in a microwave oven. Pollen grains from three flowers were spread on the surface of 250 μl agarose germination pads on microscope slides covered by polypropylene foil by inverting the flower with the help of tweezers and gently bringing it onto agarose surface. The whole flower was used as a 'brush' to spread pollen uniformly. The slides were incubated upside down in a moisture incubation chamber for 16 h in the dark at 22 °C and 100% humidity. The samples were examined by bright-field microscopy using Nikon TE2000-E microscope (objective Nikon CFI Plan UW 2×/0.06, eyepiece Nikon CFI 10×/22, intermediate magnification ×1–×1.5). The germinating pollen was defined as a pollen with a clearly visible pollen tube with length at least 1 diameter of pollen grain. The germination was carried out overnight (16 h). The percentage of germinated pollen was scored manually from captured image. From each microscope slide, five to six individual areas were taken. For NAA pollen germination test, 1 μM NAA was dissolved in the germination medium to 100 nM final concentration.

References

- Leyser, O. The power of auxin in plants. *Plant Physiol.* **154**, 501–505 (2010).
- Leyser, O. Auxin distribution and plant pattern formation: how many angels can dance on the point of PIN? *Cell* **121**, 819–822 (2005).
- Santner, A. & Estelle, M. Recent advances and emerging trends in plant hormone signalling. *Nature* **459**, 1071–1078 (2009).
- Kepinski, S. & Leyser, O. Plant development: auxin in loops. *Curr. Biol.* **15**, R208–210 (2005).
- Chapman, E. J. & Estelle, M. Mechanism of auxin-regulated gene expression in plants. *Annu. Rev. Genet.* **43**, 265–285 (2009).
- Woodward, A. W. & Bartel, B. Auxin: regulation, action, and interaction. *Ann. Bot.* **95**, 707–735 (2005).
- Grunewald, W. & Friml, J. The march of the PINs: developmental plasticity by dynamic polar targeting in plant cells. *EMBO J.* **29**, 2700–2714 (2010).
- Vanneste, S. & Friml, J. Auxin: a trigger for change in plant development. *Cell* **136**, 1005–1016 (2009).
- Pagnussat, G. C., Alandete-Saez, M., Bowman, J. L. & Sundaresan, V. Auxin-dependent patterning and gamete specification in the Arabidopsis female gametophyte. *Science* **324**, 1684–1689 (2009).
- Wu, M.-F., Tian, Q. & Reed, J. W. Arabidopsis microRNA167 controls patterns of ARF6 and ARF8 expression, and regulates both female and male reproduction. *Development* **133**, 4211–4218 (2006).
- Feng, X.-L. *et al.* Auxin flow in anther filaments is critical for pollen grain development through regulating pollen mitosis. *Plant Mol. Biol.* **61**, 215–226 (2006).
- Cecchetti, V., Altamura, M. M., Falasca, G., Costantino, P. & Cardarelli, M. Auxin regulates Arabidopsis anther dehiscence, pollen maturation, and filament elongation. *Plant Cell* **20**, 1760–1774 (2008).
- Chen, D. & Zhao, J. Free IAA in stigmas and styles during pollen germination and pollen tube growth of Nicotiana tabacum. *Physiol. Plant* **134**, 202–215 (2008).
- Zhao, Y. Auxin biosynthesis and its role in plant development. *Annu. Rev. Plant Biol.* **61**, 49–64 (2010).
- Stepanova, A. N. *et al.* TAA1-mediated auxin biosynthesis is essential for hormone crosstalk and plant development. *Cell* **133**, 177–191 (2008).
- Ikeda, Y. *et al.* Local auxin biosynthesis modulates gradient-directed planar polarity in Arabidopsis. *Nat. Cell Biol.* **11**, 731–8 (2008).
- Petrásek, J. & Friml, J. Auxin transport routes in plant development. *Development* **136**, 2675–2688 (2009).
- Swarup, R. & Bennett, M. Auxin transport: the fountain of life in plants? *Dev. Cell* **5**, 824–826 (2003).
- Swarup, K. *et al.* The auxin influx carrier LAX3 promotes lateral root emergence. *Nat. Cell Biol.* **10**, 946–954 (2008).
- Petrásek, J. *et al.* PIN proteins perform a rate-limiting function in cellular auxin efflux. *Science* **312**, 914–918 (2006).
- Noh, B., Murphy, A. S. & Spalding, E. P. Multidrug resistance-like genes of Arabidopsis required for auxin transport and auxin-mediated development. *Plant Cell* **13**, 2441–2454 (2001).
- Geisler, M. *et al.* Cellular efflux of auxin catalyzed by the Arabidopsis MDR/PGP transporter AtPGP1. *Plant J.* **44**, 179–94 (2005).
- Křeček, P. *et al.* The PIN-FORMED (PIN) protein family of auxin transporters. *Genome Biol.* **10**, 249–256 (2009).
- Mravec, J. *et al.* Subcellular homeostasis of phytohormone auxin is mediated by the ER-localized PIN5 transporter. *Nature* **459**, 1136–1140 (2009).
- Dupáková, N. *et al.* Arabidopsis Gene Family Profiler (aGFP)–user-oriented transcriptomic database with easy-to-use graphic interface. *BMC Plant Biol.* **7**, 39: 10.1186/1471-2229-7-39 (2007).
- Peer, W. A. *et al.* Mutation of the membrane-associated M1 protease APM1 results in distinct embryonic and seedling developmental defects in Arabidopsis. *Plant Cell* **21**, 1693–1721 (2009).
- Sánchez-Morán, E. *et al.* A puromycin-sensitive aminopeptidase is essential for meiosis in Arabidopsis thaliana. *Plant Cell* **16**, 2895–909 (2004).
- Ishikawa, F., Suga, S., Uemura, T., Sato, M. H. & Maeshima, M. Novel type aquaporin SIPs are mainly localized to the ER membrane and show cell-specific expression in Arabidopsis thaliana. *FEBS Lett.* **579**, 5814–5820 (2005).
- Ulmasov, T., Liu, Z. B., Hagen, G. & Guilfoyle, T. J. Composite structure of auxin response elements. *Plant Cell* **7**, 1611–1623 (1995).
- Reyes, F., León, G., Donoso, M., Brandizzi, F., Weber, A. P. & Orellana, A. The nucleotide sugar transporters AtUTR1 and AtUTR3 are required for the incorporation of UDP-glucose into the endoplasmic reticulum, are essential for pollen development and are needed for embryo sac progress in Arabidopsis thaliana. *Plant J.* **61**, 423–35 (2010).
- Ganguly, A. *et al.* Differential auxin-transporting activities of PIN-FORMED proteins in Arabidopsis root hair cells. *Plant Physiol.* **153**, 1046–1061 (2010).
- Aloni, R., Aloni, E., Langhans, M. & Ullrich, C. I. Role of auxin in regulating Arabidopsis flower development. *Planta* **223**, 315–328 (2006).
- Friml, J. *et al.* Efflux-dependent auxin gradients establish the apical-basal axis of Arabidopsis. *Nature* **426**, 147–153 (2003).
- Weijers, D. *et al.* Maintenance of embryonic auxin distribution for apical-basal patterning by PIN-FORMED-dependent auxin transport in Arabidopsis. *Plant Cell* **17**, 2517–2526 (2005).
- Benková, E. *et al.* Local, efflux-dependent auxin gradients as a common module for plant organ formation. *Cell* **115**, 591–602 (2003).
- Sauer, M., Paciorek, T., Benková, E. & Friml, J. Immunocytochemical techniques for whole mount *in situ* protein localization in plants. *Nat. Protoc.* **1**, 98–103 (2006).
- Pencik, A. *et al.* Isolation of novel indole-3-acetic acid conjugates by immunoaffinity extraction. *Talanta* **80**, 651–655 (2009).
- Munoz, P., Norambuena, L. & Orellana, A. Evidence for a UDP-glucose transporter in Golgi apparatus-derived vesicles from pea and its possible role in polysaccharide biosynthesis. *Plant Physiol.* **112**, 1585–1594 (1996).
- Liang, F. & Sze, H. A high-affinity Ca²⁺ pump, ECA1, from the endoplasmic reticulum is inhibited by cyclopiazonic acid but not by thapsigargin. *Plant Physiol.* **118**, 817–825 (1998).
- Ding, Z. J. *et al.* Auxin regulates distal stem cell differentiation in Arabidopsis roots. *Proc. Natl Acad. Sci. USA* **107**, 12046–120 (2010).
- Park, S. K., Howden, R. & Twell, D. The Arabidopsis thaliana gametophytic mutation gemini pollen disrupts microspore polarity, division asymmetry and pollen cell fate. *Development* **125**, 3789–3799 (1998).
- Boavida, L. C. & McCormick, S. Temperature as a determinant factor for increased and reproducible *in vitro* pollen germination in Arabidopsis thaliana. *Plant J.* **52**, 570–582 (2007).

Acknowledgements

We thank Vincent Vincenzetti, Laurence Charrier and Jinsheng Zhu for help with yeast and tobacco transport assays; Markéta Pařezová for BY-2 cell line transformations and maintenance; Klára Hoyerová and Petre I. Dobrev for help with metabolic profiling. This work was supported by the funding from the projects CZ.1.07/2.3.00/20.0043 and CZ.1.05/1.1.00/02.0068 (to CEITEC, Central European Institute of Technology) and the Odysseus program of the Research Foundation-Flanders to J.F., from 'Qilu Scholarship' of Shandong University (11200081963024) to Z.D., from German Science Foundation (DFG-SFB480/A-10) to S.P., from Swiss National Science Foundation (Grant No. 31003A-125001) and Forschungspool of the University of Fribourg to M.G., from the Ministry of Education, Youth and Sports of the Czech Republic, projects LC06034 to P.S., J.P. and E.Z., KAN200380801 to J.R. (Jakub Rolčík), and OC10054 to N.D., from the Czech Science Foundation (522/09/0858) to D.H., ICM-P10-062-F, Basal Program PFB-16, FONDAP-CRG to A.O. and NSF-IOS (0820648) to A.S.M.

Author contributions

J.F., Z.D., A.M. and M.G. planned experiments. B.W., N.D., S.S., P.S., A.P., S.P., J.M., X.C., I.M., N.C., J.R. (Jesica Reemmer) and Z.D. performed experiments. J.F., Z.D., M.G., D.H., J.P., J.R. (Jakub Rolčík), X.C., I.M., A.O., R.T. and E.Z. analysed the data. J.F. and Z.D. wrote the paper. All authors discussed the results and commented on the manuscript.

Additional information

Supplementary Information accompanies this paper at <http://www.nature.com/naturecommunications>

Competing financial interests: The authors declare no competing financial interests.

Reprints and permission information is available online at <http://npg.nature.com/reprintsandpermissions/>

How to cite this article: Ding, Z. *et al.* ER-localized auxin transporter PIN8 regulates auxin homeostasis and male gametophyte development in *Arabidopsis*. *Nat. Commun.* 3:941 doi: 10.1038/ncomms1941 (2012).

License: This work is licensed under a Creative Commons Attribution-NonCommercial-NoDerivative Works 3.0 Unported License. To view a copy of this license, visit <http://creativecommons.org/licenses/by-nc-nd/3.0/>